International Journal Of Engineering Research And Development
e- ISSN: 2278-067X, p-ISSN: 2278-800X, www.ijerd.com
Volume 18, Issue 3 (May.-June. 2022), PP. 25-47

Techno-Economical Optimization of Renewable Energy Resources in Hybrid Energy Systems

Mona M. Algaml[1,A], Zeinab H. Osman, SLIEEE member [1,b], and Mostafa A. Elshahed [1,2,c, *]

[1]*Electrical Power Engineering, Faculty of Engineering, Cairo University, Giza, Egypt*
[2]*Electrical Engineering, College of Engineering and Information Technology, Buraydah Private Colleges, Buraydah, KSA*
Corresponding Author: Mostafa A. Elshahed m.elshahed@eng.cu.edu.eg

ABSTRACT: *The massive increase in energy demand, the deficiency of natural resources, and the recent world awareness of improving environmental conditions are the master reason behind the utilization of Renewable Energy Resources (RERs). Optimizing RERs in Hybrid Energy Systems (HESs) is a multiobjective problem considering economic, technical, and environmental issues. This paper develops a procedure to optimize the solution of standalone or grid-connected HESs. The formulations of the objective function, unit, and system constraints are clarified. For verification, the procedure is applied to a selected irrigation project in Upper Egypt by implementing HOMER software to optimize the RERs for reliable and economical feeding HES. Groups of irrigation, domestic, and welding loads are considered in the study as built in the project. Twelve HESs are investigated to supply the practical load profile to deduce general guidelines for optimizing RERs in other projects. The TOPSIS is utilized to rank the different alternatives of HESs based on various criteria. The study results show that the utilization of RERs in the HESs is suitable for achieving global sustainable energy development.*

Keywords: Renewable Energy Resources; Energy Storage System; Hybrid Energy Systems; Techno-economical Optimization; TOPSIS

Date of Submission: 13-06-2022 Date of Acceptance: 27-06-2022

Abbreviations

COE	Cost of energy	PSO	Particle Swarm Optimization
ESS	Energy Storage System	PV	Photovoltaic
GHI	Global Horizontal Irradiance	REF	Renewable Energy Fraction
HESs	Hybrid Energy Systems	RERs	Renewable Energy Resources
HOMER	Hybrid Optimization of Multiple Energy Resources	SOC STC	State of Charge Standard Test Condition
NPC	Net Present Cost	STP	Standard Temperature and Pressure
NREL	National Renewable Energy Laboratory	TOPSIS	Technique for Order of Preference by Similarity to Ideal Solution
		WS	Wind Speed
		WT	Wind Turbine
O&M	Operating and Maintenance Cost		

Symbols

A_{pv}	The surface area of the PV module [m^2]
$C_{ann,tot}$	Total Annualized Cost [$/yr] .
$C_{NPC,tot}$	Total net present cost (NPC) [$].
$C_{power,\ i}$	The grid power price for rate i [$/kWh]
CRF	A function returning the capital recovery factor.
$C_{sell\text{-}back,\ i}$	The sell-back price for rate i [$/kWh]
$E_{battery}$	Total annual energy output from the battery [kWh/yr]
E_{demand}	Total electrical demand (primary and deferrable load) [kWh/yr]
$E_{G,\ diesel}$	Total annual energy production of the DG [kWh/yr]
$E_{G,\ PV}$	Total annual energy production of the PV [kWh/yr]
$E_{G,\ w}$	Total annual energy production of the WT [kWh/yr]
$E_{netgridpurchases,\ i}$	The annual net grid purchases during the time that rate i applies [kWh]

E_{served}	Total electrical load served [kWh/yr]
E_{total}	The total annual energy production
$F_{\circ}$	The fuel curve intercept coefficient [units/hr/kW]
F_1	The fuel curve slope [units/hr/kW]
f_{cs}	The capacity shortage fraction [unit less]
f_{csm}	The maximum allowable value of the capacity shortage fraction.
f_{pv}	PV Derating Factor [%]
$G_{T,STC}$	The incident radiation at standard test conditions [1 kW/m2].
G_T	The solar radiation incident on the PV array in the current time step [kW/m2]
i	Annual discount rate [%]
N	Number of years
$P_{battery}$	The average output power of the battery in the current time step [kW]
$P_{G,\ diesel}$	The average output power of the diesel generator in the current time step [kW]
$P_{G,\ grid\ purchases}$	The average output power purchased from the grid in the current time step [kW]
$P_{G,\ WT}$	The average output power of the WT in the current time step [kW]
$P_{G,pv}$	The average output power of the PV array in the current time step [kW]
P_i	The performance score
P_{gen}	Electrical generator output [kW]
P_{pv}	The average PV array output in the current time step [kW]
P_{ren}	Total renewable electrical output power in this time step [kW]
$P_{WT,\ STP}$	The wind turbine power output at standard temperature and pressure [kW]
P_{WT}	The wind turbine power output [kW]
$T_{c,STC}$	The PV cell temperature under standard test conditions [25 °C]
T_c	The PV cell temperature in the current time step [°C].
U_{anem}	The wind speed at anemometer height [m/s]
U_{hub}	The wind speed at the hub height of the wind turbine [m/s]
V	Battery internal voltage in (volt)
$V_{\circ}$	Battery terminal voltage in (Volt)
Y_{pv}	The rated capacity of the PV array [kW]
$Z_{\circ}$	The surface roughness length [m]
Z_{hub}	The hub height of the wind turbine [m]
α_c	The storage's maximum charge rate [A/Ah]
$\eta_{batt,c}$	Battery charge efficiency[%]
$\eta_{batt,d}$	Battery discharge efficiency [%]
$\eta_{batt,\ rt}$	Battery round-trip efficiency[%]
$\eta_{mp,\ STC}$	The efficiency of the PV module under standard test conditions [%]
ρ	The actual air density [kg/m^3]
$\rho_{\circ}$	The air density at standard temperature and pressure (1.225 kg/m^3)

I. INTRODUCTION

The world is directed to use renewable energy resources (RERs) to produce electricity to meet the desired load instead of using conventional energy resources, such as petroleum, gas, and coal. We cannot depend on these nonrenewable resources that will be decreased in the future and pollute the environment due to the emitted emissions. Using reliable and economically effective combination units of the small-scale generation, the emission of the traditional power plants and the high cost of supplying electricity to remote areas are reduced [1]-[2]. The most populated countries cannot meet the demand of remote areas throughout the year using traditional power stations only. Thus, the Hybrid Energy System (HES) is composed of integrating RESs with traditional plants. HESs are usually optimally designed as a group of RERs such as photovoltaic (PV), Wind, Diesel, Battery, Hydro, and Flywheel. Then it is proven to be more economical and reliable than conventional energy systems.

HESs are substantially adopted for their efficient potential. The HESs design requires precise attention to achieve optimum integration between various energy sources. Due to the complex nature of several RERs, the optimum design of the HESs with suitable system sizing and appropriate energy management strategy is critical to ensure continuity of power supply and minimize the cost of energy (COE) produced and ensure protection for all system components from the damage. Wide works have taken place in integrating various RERs to design convenient HES. The configuration of the (PV-Wind) is considered the most reputable HES. On the other hand, this system must be associated with the Energy Storage System (ESS), such as batteries and/or diesel generator, to satisfy the load when there is no PV or wind.

The (PV-Wind) HES has been supplemented by diesel generators that are handled by [3] to meet commercial building requirements in KSA by Hybrid Optimization of Multiple Energy Resources (HOMER) software. A (PV-Wind-Hydro)HES has been modeled and proposed in three different regions of Ghana in [4] to optimize the cost of RERs and the COE from the consumer perspective by MATLAB. Furthermore, the Authors in [5] have integrated a backup source and ESS with a (PV-Wind) HES to supply a seasonal electric demand. In [6], the economic benefits of the (PV-Wind) HES grid-tie have been maximized at four different locations in Ireland using particle swarm optimization (PSO). A maximum power point tracking algorithm for (PV-Wind) HES has been developed in [7] to satisfy an isolated resort island west of Malaysia. In [8], a climatological study has been accomplished to discover the co-variability of the irradiance and the wind speed (WS) over Britain based on the average daily irradiance and WS. Moreover, the impact of this correlation on the energy supplied has been investigated.

A (PV-Wind-Battery) HES has been proposed in [9] and simulated by MATLAB and HOMER to meet the irrigation and domestic loads for a farm in TOSKKA in Egypt. In [10], (PV-Wind-Battery), (Wind-Battery), and (PV-Battery) HESs have been optimized by HOMER software. The lowest Net Present Cost (NPC) has been achieved by the (PV-Wind-Battery) HES. Furthermore, a sensitivity analysis has been performed for the grid extension and its effect on NPC. Reference [11] optimized (PV-Wind-Battery) HES by HOMER software to serve an annual load consumption in Tunisia and performed a sensitivity analysis for the battery and converter sizes. Additionally, a second sensitivity analysis has been performed for the diesel size and the fuel price. The generation adequacy for micro-grid has been employed in [12] to feed a residential load from conventional generation and RERs (PV-Wind) optimally sized by PSO, considering minimizing the total system cost and unmet loads.

Modeling of the (PV-Wind-Battery) HES has been considered in [13] to meet the electric demand in Jazan province, KSA. An intelligent graphical user interface has been established to model, simulate, and monitor a standalone system. In [14], a Genetic Algorithm has been used for optimizing the configuration of (PV-Wind-Hydro-Diesel-Battery) standalone HES at the minimum cost of the system. Three configuration systems are modeled in [15]; (PV-Wind-Diesel), (PV-Diesel), and (Wind-Diesel) HESs. Moreover, a deterministic algorithm has been conducted to optimize the size and the number of all system components to ensure the minimum cost of the system configuration and minimize the unmet load. The (PV-Wind-Diesel) HES has the least NPC. In [16], a (PV-Wind-Diesel) standalone HES configuration has been used to achieve the least cost and enhance the system's safety and reliability. The approach of a hybrid multiobjective PSO has been suggested in [17] for the economic allocation of ESS in distribution systems incorporating RERs. Standalone HESs have been investigated for a remote area in South Australia [18] by the approach of a PSO to achieve the least NPC over a 20-year lifespan.

Reference [19] has explored the application of (PV-Wind-Battery) in a microgrid system to minimize the total annual cost and environmental impact reduction index using MATLAB toolboxes. The economic effect of using wind energy in ten locations in South Africa based on the planned grid has been investigated in [20] by HOMER software to assess the wind energy on provincial and national scales, along with estimating the annual energy generation of the selected locations. Reference [21] has introduced an accurate iterative methodology for optimal sizing of a (PV-Wind) HES with ESS using the concept of the loss of power supply probability and the NPC. On the other hand, due to the rapid increase in electricity consumption, there is a tendency to install DGs driven by RERs at the level of distribution systems [22]. With the increasing penetration of RERs in distribution systems, there is a need to analyze fault currents [23], voltage profile, power flow, power losses, and voltage stability [24].

This paper develops a techno-economic and environmental feasibility procedure based on the HOMER software's optimization analysis technique. Twelve configurations are carried out to meet the Irrigation, Administrative, Domestic and Welding loads of a farm in Tushka, Egypt. From the obtained results, general guidelines for optimizing RERs in other projects are deduced. This paper is structured as follows; section 2 introduces mathematical modeling of the HES components. In section 3, the optimization problem formulation where the objective functions and system constraints are described. Section 4 introduces the proposed procedure for optimizing the RERs in HESs. Sections 5 and 6 introduce the techno-economical results with discussions of the considered configurations. Section 7 concludes the distinctive feature of the HES performance and the optimal HES configurations and suggests a future research topic.

II. MODELING OF THE SYSTEM COMPONENTS

The modeling of the system components is briefly presented in this section. The power generators are classified into two types: dispatchable and non-dispatchable. The dispatched power generators are controllable resources. Their output power can be adjusted in contrast with the non-dispatched power generators.

2.1 PV System:

PV array is regarded as a device that produces DC electricity directly to the Global Horizontal irradiance (GHI) upon it. The GHI is calculated for every time step in the simulation. The PV array output power (P_{pv}) counts on the quantity of solar radiation striking the array (which may not be horizontally located). In each time step, the solar radiation incident on the surface of the PV array must be calculated. The output power of the PV array is calculated by (1) [25], [26].

$$P_{pv} = Y_{pv} * f_{pv} * \left[\frac{\bar{G}_T}{\bar{G}_{T,STC}}\right] * \left[1 + \alpha_p(T_c - T_{c,STC})\right] \quad (1)$$

The PV array is rated at standard test conditions [27] (STC), which are the radiation of 1kW/m^2 ($G_{T,STC}$), cell temperature of 25˚C ($T_{c,STC}$), and no wind. Moreover, the ambient temperature effect on the panel's efficiency is considered. The selected PV is a Generic flat plate [25] with a rated capacity of 1 kW, with no tracking system, and its derating factor is 80 %. The PV efficiency is set at STC and given by (2).

$$\eta_{mp,STC} = \frac{Y_{pv}}{A_{pv} * G_{T,STC}} \quad (2)$$

Where A_{pv} is the surface area of the PV module in m^2, Y_{pv} is the rated kW capacity of the PV array.

2.2 Wind Turbine (WT) System:

Wind Turbine (WT) is modeled as a device that converts the wind kinetic energy into AC or DC electricity based on a particular power curve, which is a graph of the wind output power versus WS at a certain hub height (the rotor's height above the ground). The Generic 3kWWT is selected based on the wind characteristic [28], with a hub height of 25 meters and a lifetime of 20 years. To calculate the output power of the WT at every time step, there are three-step that should be followed:

- Calculating the WS at the particular hub height of the WT.
- Then, determining the WT output power at that WS at standard air density.
- Lastly, adjusting the value of the output power for the actual air density by multiplying the output power by the air density ratio (ρ/ρ_o).

The air density ($\rho_\circ$) at standard temperature and pressure (STP) is 1.225 kg/m^3.

A synthetic WS data-synthesis algorithm is used where the equation (3) [29] is utilized to evaluate the WS hub height (U_{hub}) to create time-step WS data.

$$U_{hub} = U_{anem} * \frac{\ln\left(\frac{Z_{hub}}{Z_\circ}\right)}{\ln\left(\frac{Z_{hub}}{Z_\circ}\right)} \quad (3)$$

$Z_\circ$ is a factor that characterizes the roughness of the surrounding terrain; its value is typically between0.00001m to 3.0m [29].

The power curve specifies the performance of the WT under the STP. To modify the output power at the actual condition (P_{WTG} in kW), equation (4) [26] is utilized.

$$P_{WTG} = \left[\frac{\rho}{\rho_o}\right] * P_{WTG,STP} \quad (4)$$

2.3 Diesel Generator:

A generator consumes fuel to generate electricity and probably heat as a side-product. It is considered a dispatchable source, meaning the system operates when necessary. Auto-sized Genest (Generic manufacturer) is selected [25].It is assumed that the generator fuel curve is represented as a straight line. This curve is given by the fuel consumption in [30].

$$F = F_\circ * Y_{gen} + F_1 * P_{gen} \quad (5)$$

The generator fuel curve intercept coefficient $F_\circ$ represents the no-load fuel consumption of the generator divided by the generator rated capacity Y_{gen}. In contrast, the generator fuel curve slope F_1 is defined as the generator marginal fuel consumption.

2.4 Battery System:

The Batteries primarily support excess or lack of energy, ensuring a reliable and stable energy system [31]. For short and mid-term electricity storage, the Lead Acid batteries are most commonly used because they are used for storage in small and medium-scale energy systems to control the problem of short-term energy shortage. The type of battery selected is the Kinetic Battery Model (Generic 12 V lead Acid battery with 1 kWh of energy storage). This type of battery is chosen due to its good performance and low cost [27], [32]. The lead-Acid battery consists of a two-tank system to separate the available electricity produced from the chemical bond energy that cannot be utilized [33], [34]. The Lead-Acid battery is modeled as a voltage source connected in series with constant resistance $R_\circ$ that is assumed to be constant, and the internal voltage V varies with the battery's state of charge. Besides, the current regulator is placed between the battery and the load to guarantee a

fixed current and drown power over time. For a given current I and a battery terminal voltage V [35], the output power is defined as in (6).

$$P_{out} = V * I_{out} = V_{\circ} * I - R_{\circ} * I^2 \quad (6)$$

Then, this current is implemented in the ESS model to specify the state for the post-mentioned time step. It is considered that the battery storage charge $\eta_{batt,c,}$ and discharge $\eta_{batt,d}$ efficiencies are equal to the root mean square of the battery round-trip efficiency $\eta_{batt,\ rt}$ (is the round-trip DC-to-storage-to-DC energy efficiency of the ESS) as illustrated in (7).

$$\eta_{batt,c} = \eta_{batt,d} = \sqrt{\eta_{batt,rt}} \quad (7)$$

In this study, when the ESSs are fully charged, the battery state of charge (SOC) is equal to the maximum capacity of the ESS. The relative SOC (is the ratio of the current absolute SOC to the maximum capacity of the ESS)is 100 %.

2.5 Converter

The suggested HES consists of both AC and DC systems. Thus, a power converter is required to control the flow of power between the system and the load. The selected type of converter is a Generic system converter with a capacity of 100 kW. The relative capacity of the rectifier is defined as its rated capacity relative to that of the inverter in percentage.

2.6 Grid-Parameters

The selected billing system is the Net metering billing scheme. In this billing system, the utility allows the subscriber to sell power to the grid at the retail rate. Whenever surplus power exists, the meter runs backward by which the surplus power is sold to the grid. It is important to define the sale and purchase capacity; the sale capacity is the maximum power (kW) that can be sold back to the grid at any time step, while the purchasing capacity is the maximum power that can be purchased from the grid in any time-step. Moreover, purchase capacity is considered an optimization input that can reduce the demand charges for peak shaving systems. The total annual energy-charged (the Net generation is calculated annually) is calculated by (8) [25].

$$C_{grid,energy} = \sum_i^{rate} \begin{cases} E_{netgridpurchases,i} * C_{power,i} & if\ E_{netgridpurchases,i} \geq 0 \\ E_{netgridpurchases,i} * C_{sellback,i} & if\ E_{netgridpurchases,i} < 0 \end{cases} \quad (8)$$

The annual net grid purchases $E_{netgridpurchases,\ i}$ is the average net energy purchased from the grid (kWh) during the time that rate "i" applies (which equals grid purchases – grid sales). The grid purchases are defined as the total average energy purchased from the grid, while the grid sale is defined as the total average energy sold to the grid.

III. OPTIMIZATION PROBLEM FORMULATION

3.1 Main Objective Function

The main objective function is to minimize the NPC of the configuration, as illustrated in (9).

$$\{\text{Min}\ (C_{\text{NPC,tot}})\} \quad (9)$$

The NPC is given by the sum of all system components' present value (which includes the capital cost, replacement cost, operating and maintenance (O&M) cost, fuel cost, penalty (emission and capacity shortage penalties), and the cost of purchasing power from the grid) over its lifespan minus the present value of the revenue (includes the salvage value and grid sales revenues) that earns throughout its lifespan. The total NPC is given by (10) [25].

$$C_{NPC,tot} = \frac{C_{ann,tot}}{CRF(i,R_{proj})} \quad (10)$$

CRF is given by (11) [25].

$$CRF(i,N) = \frac{i(1+N)^N}{(1+i)^N - 1} \quad (11)$$

3.2 Other Objective Function

The Levelized Cost of Energy is defined as the average cost per kWh of the useful electricity that the system produces. It is given by (12).

$$\{\text{Min}(\text{COE})\} \quad (12)$$

3.3 Power and Energy BalanceConstraints

This constraint explains the energy and power flow of the system. At each time, the power production (kW) should meet the load as illustrated by (13), (14) [30], [32].

$$P_{demand} = P_{G,\ pv} + P_{G,\ W} + P_{G,\ diesel} \text{ or } P_{G,\ gridpurchases} \text{ or } P_{battery} \quad (13)$$

Therefore, the time-step energy Constraint throughout the whole year

$$E_{demand} = E_{G,\,PV} + E_{G,\,w} + E_{G,\,diesel} \text{ or } E_{G,\,gridpurchases} \text{ or } E_{battery} \quad (14)$$

3.4 Generation LimitConstraints

The total annual energy production (E_{total}) from all power sources of the system throughout the year is greater than or equal to the total annual energy load served.

$$E_{total} \geq E_{served} \quad (15)$$

The output power of the PV constraint is limited between two boundaries given by (16)[18], [36].

$$0 \leq Ppv \leq Ppv_{,\,max} \quad (16)$$

The WT output power constraint is given by (17) [18], [37].

$$0 \leq P_{WT} \leq P_{WT,\,max} \quad (17)$$

The output power of the diesel generator is given by (18) [18].

$$P_{gen,\,min} \leq P_{gen} \leq P_{gen,\,max} \quad (18)$$

The BESS constraint is given by (19) [37].

$$SOC_{min} \leq SOC \leq SOC_{max} \quad (19)$$

It is recommended to consider the minimum state of charge (typically 30-50 %) [38]. It is the relative SOC below which the ESS is never drawn.

3.5 Capacity Shortage Constraint

f_{cs} is the total amount of capacity shortage that occurred over the year (it is the shortfall between the required operating capacity and the actual operating capacity provided by the power sources at every time interval), and f_{csm} is the maximum allowable annual capacity shortage fraction [39].

$$f_{cs} \leq f_{csm} \quad (20)$$

3.6 Operating Reserve Constraint

This constraint ensures a reliable power supply even if the load suddenly increases or the sustainable power output decreases [39]. It is illustrated as follows:

$$Operating\ reserve \geq required\ operating\ reserve \quad (21)$$

$$Operating\ reserve = operating\ capacity - electric\ load\ deamand \quad (22)$$

3.7 System Dispatch Strategy Constraint

The controllable power sources (grid, generator, and ESS) are dispatched to supply the AC primary load, and charging ESS is left to the renewable power sources under the least total cost at each time-step while meeting the operating reserve demand [33], [40].

3.8 Minimum Renewable Energy Fraction (REF) Constraint

REF represents the minimum acceptable value of the produced energy from RERs.

IV. PROPOSED PROCEDURE BASED ON HOMER SOFTWARE

HOMER is a computer software [41] advanced by the US National Renewable Energy Laboratory (NREL). It models the physical behavior of the power system and the total cost value of installing and operating the system during its lifespan. Additionally, it facilitates comparing different technical or economic designs based on their merits. The proposed procedure based on HOMER software to optimize the RERs for reliable and economical HES is shown in Figure 1. The more specific inputs that describe the component costs, the technology options, and the resource availability provided to the model, the more accurate optimization solution is obtained. Then, a simulation analysis is carried out for different system configurations using the predetermined inputs. Finally, the results are generated and listed as feasible configurations sorted by the NPC (lifecycle cost). A sensitivity analysis is implemented when studying the effect of the uncertainty or changes in factors or variables that are not controlled. For example, system resource availability (average WS) and economic conditions (the future fuel price in the design and operation of the power system to inform planning and policy decisions).

V. RESULTS AND DISCUSSIONS

5.1 Case Study data

The proposed procedure is applied for a selected irrigation project in Upper Egypt by implementing HOMER software to optimize the RERs for reliable and economical feeding HES. Groups of irrigation, domestic, and welding loads are considered in the study as built in the project. In this project, there are two types of AC Electric Loads; Main Loads which are the irrigation load which includes the Pumping and Motor System, and Secondary Loads are the Administrative, Domestic, and welding loads. These electric loads will be

symbolized by "A primary electric load," which has the priority to be supplied with electric energy in case of a supply deficiency. The average load measurements recorded daily in the project are given in Figure 2. Table 1 contains the daily consumption data based on the recorded measurements built in the project.

However, the random variability inputs allow using randomness to load data to obtain real data. Random variability inputs are Day-to-Day (where the value and shape of the load change from one day to another) and time step (which changes the shape of the load profile). Table 2 lists these variability inputs. Figure 3 shows a box plot of the monthly average load profile, each box (which identifies each month) contains five values, the maximum load consumption recorded during this month, the minimum value recorded, the average value recorded, the daily average maximum value, and daily average minimum value. Appendix A shows the detailed data of the considered project.

The discount rate, inflation rate, the maximum allowable capacity shortage per year, and the project lifetime as basic data for HOMER in Table 3. These data are used as general data entry to Homer Simulation Program in all cases. All possible HES configurations are investigated to supply the practical load profile to determine the optimal feeding configuration. Twelve configurations are investigated as follows:

I. (PV) Grid-Connected HES.
II. (PV-Diesel) Standalone HES.
III. (PV-Battery) Standalone HES.
IV. (PV-Diesel-Battery) Standalone HES.
V. (Wind-Diesel) Standalone HES.
VI. (Wind-Battery) Standalone HES.
VII. (Wind-Diesel-Battery) Standalone HES.
VIII. (PV-Wind-Diesel) Standalone HES.
IX. (PV-Wind-Battery) Standalone HES.
X. (PV-Battery-Wind-Diesel) Standalone HES.
XI. (PV-Wind) Grid-Connected HES.
XII. (Wind)Grid-Connected HES.

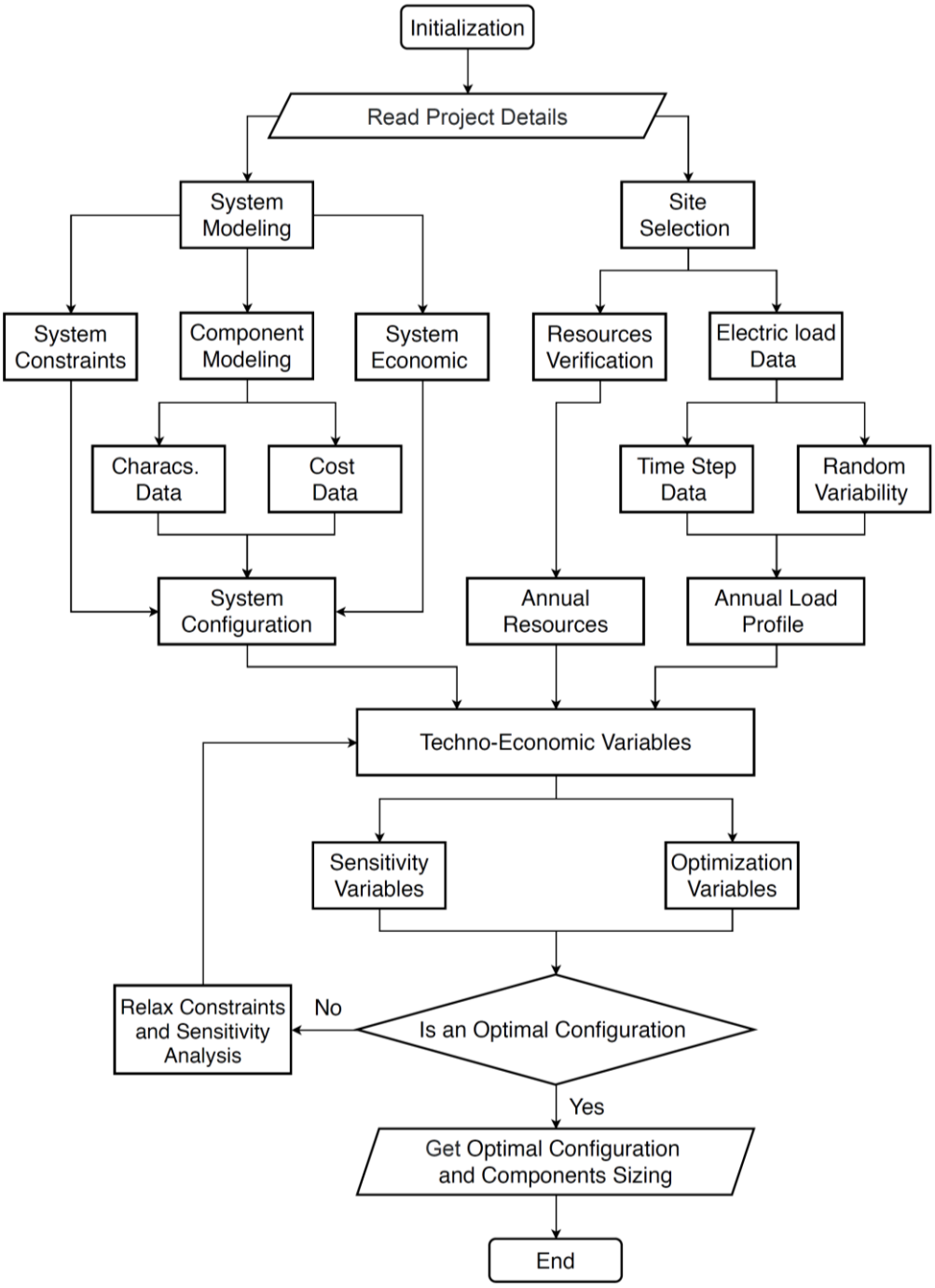

Figure 1: Flowchart of the Proposed Procedure

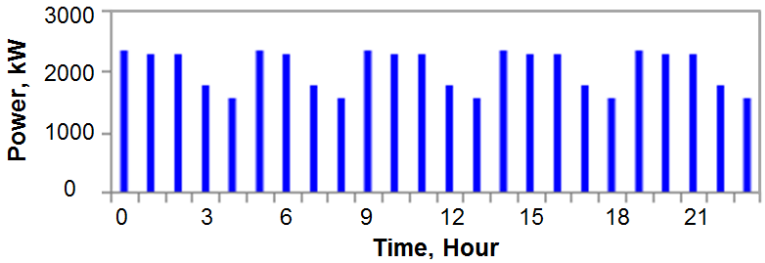

Figure 2: Average Daily Load

Table 1: Daily Load Consumption

Total average load (kWh/day)	48885
Average Load (kW)	2036.8
Peak Load(kW)	3,317.9
Load Factor	0.61

Table 2: Random Variability of Load Data

Day-to-Day %	5
Time step %	10

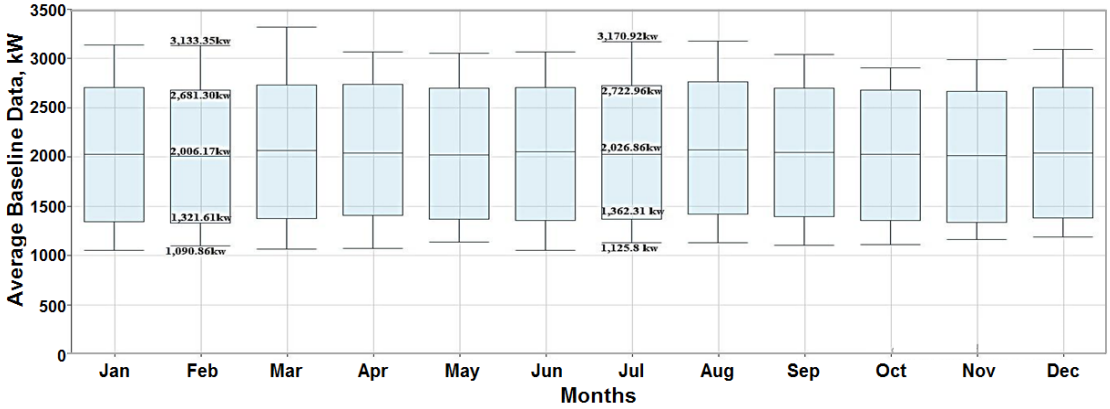

Figure 3: Average Monthly Load Profile

Table 3: Basic Data for Homer Simulation

Discount Rate %	12.75 [40]
Inflation Rate %	2 [40]
Annual Capacity shortage %	0
Project lifetime(year)	25

Three select configurations that have good results, namely (I. (PV) Grid-Connected HES, V. (Wind-Diesel) Standalone HES, and VI. (Wind-Battery) Standalone HES) are investigated in detail in this section. A comparison among the twelve configurations will be presented in Section 6.

5.2 (PV)Grid-Connected HES:

In such a case, the farm of the selected area is connected to the Grid and PV system, as shown in Figure 4.

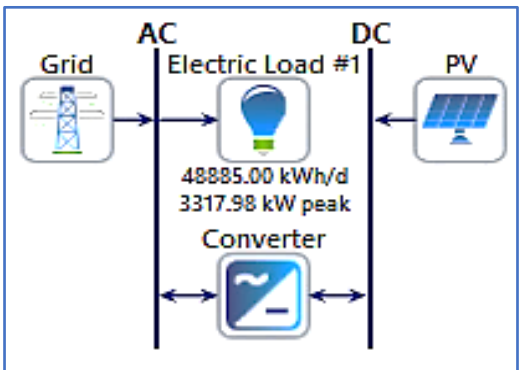

Figure 4: (PV) Grid-Connected HES (Configuration I)

The size (capacity) of the PV system will be optimized using the HOMER optimizer to satisfy the specified constraints. These constraints are:

- The power and energy balance constraints are given by equations (13) and (14) are satisfied.
- Maximum annual capacity shortage equals 0 %.
- Minimum REF greater than 0 %.
- Operating reserve as a percentage of the load in the current time step is 10 % [43].

Consequently, HOMER simulates 513 solutions; 473 are feasible based on the capacity shortage fraction f_{cs} equal to the maximum annual capacity shortage. Samples of these feasible configurations are listed in Table 4, where HOMER ranks the HES configurations according to the NPC value. Therefore, the comparison section will illustrate the optimal size of the HES components. The given size of the flat plate PV is at the standard conditions.

Table 4: Optimization Results (Configuration I)

PV (kW)	Converter (kW)	NPC ($)	COE ($)	O&M ($/yr)	Initial capital ($)	REF (%)
26479.9167	14931	7575037	0.0172	-1772006	2.30E+07	81.5191
25970.6875	14931	7576035	0.0174	-1730982	2.27E+07	81.3164
26989.1458	14931	7589325	0.0171	-1811275	2.34E+07	81.7089
25461.4583	14931	7595998	0.0176	-1687781	2.23E+07	81.0979
25716.0729	14873.9719	7598883	0.0175	-1705941	2.25E+07	81.1899
26734.5313	14873.9719	7602216	0.0172	-1787378	2.32E+07	81.5935

Figure 5 displays how the HRS reserves money within the project's lifetime and the cumulative nominal cash flow over the project lifetime. The blue line represents the optimal HES, and the black line represents the base case system (the reference system selected to be the system with the least initial capital cost). In the base case, it is considered that the grid supplies the electric demand. The simple payback in years occurs when the two lines cross each other [25], [44]. The payback equals 6.8 years. This period indicates the duration it would take to recover the difference in investment costs between the optimal HES and base case system. The cost comparison between the optimal HES and the base system based on the NPC, COE, initial cost, operating cost, and the environment effect (CO2 emitted) are given in Table 5.

The negative value of the operating cost (the annual value of all costs and revenues other than initial capital cost) represents the annual value gained related to the annual sale capacity that is sold back to the grid. The present worth value is the difference between NPC of the two system configurations (base case system and the optimal HES) is $5,640,217. The positive value represents that the optimal system reserves money throughout the project lifetime compared to the base case system. Internal rate of return (IRR) [44] is defined as the discount rate (i) at which the system base case and the optimal HES share similar NPC. In contrast, the return of investment (ROI) [44] is the average yearly difference in nominal cash flows over the project lifetime divided by the difference in capital cost. In this case, the IRR is 13.8 %, and the ROI is 10.2 %, representing the yearly cost-saving relative to the initial investment.

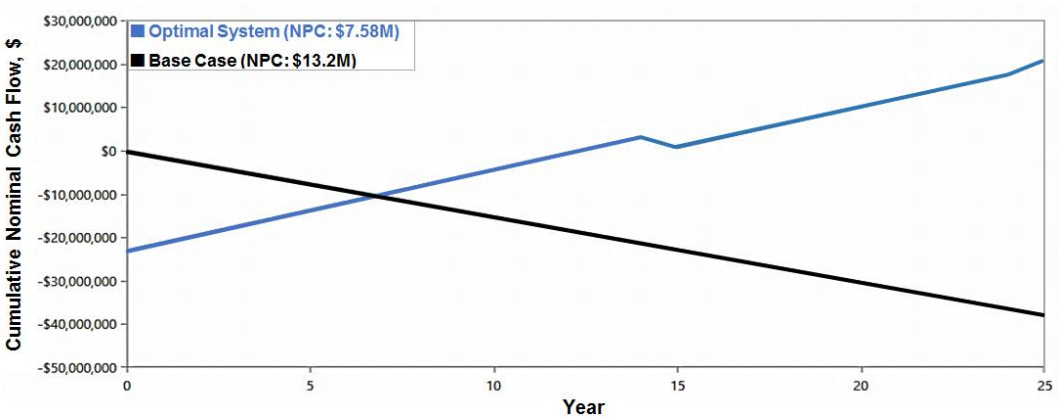

Figure 5: Cumulative Nominal Cash Flow of the Base Case and Optimal HES

Table 5: Cost Summary for Base Case and Optimal HES

	Base Case (grid-connected)	Optimal HES
NPC ($)	13.2 M	7.58 M
Initial Capital Cost ($)	0.00 M	23.0M
Operating cost ($/yr)	1.52 M	-1.77 M
Cost of Energy ($/kWh)	0.0850	0.0172
Co_2 Emitted (kg/yr)	11,276,790	5,909,888

The total electrical productions of the optimal HES are shown in Table 6. Monthly electrical production for both solar and grid during the year is shown in Figure 6. The average annual power production by the HES is 54,834,304 kWh/yr to serve the total average annual load demand of 50,598,746 kWh/yr. The total system losses of the power production are 4,235,558 kWh/yr, with 7.724% of the total production. It is lost in the DC bus and/or system inverter and/or power controller. Table 7 illustrates the PV array output, the annual average amount of power produced, and the array's capacity factor, which represents the annual average power produced compared to the rated capacity of the array and other parameters. The capacity factor of the PV array is the average output power in kW divided by the rated capacity of the PV array {(5,192.148/26,480)*100 = 19.608 %}.

Table 6: Electrical Production from PV and Grid (Configuration I)

Production	kWh/yr	%
Generic flat plate PV	45,483,216	82.9%
Grid Purchases	9,351,089	17.1%
Total	54,834,304	100

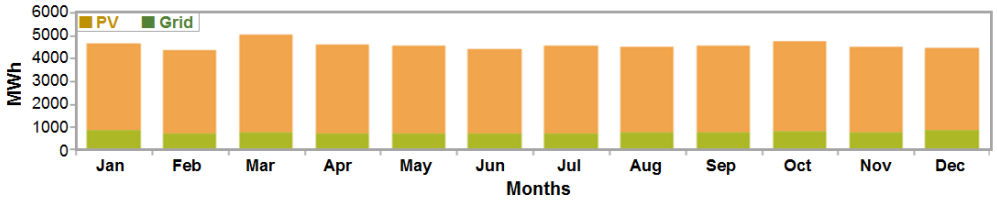

Figure 6: Monthly Electric Production of the Optimal HES (Configuration I)

Table 7: Optimal PV Outputs and Statistics (Configuration I)

Quantity	Value
Mean power output	5,192 (kW)
Mean energy output per day	124,612 (kWh/day)
Capacity factor	19.6%
Minimum output	0
Maximum output	22,169 (kW)
Hours of Operations	4,373 (hrs/yr)
Levelized Cost	0.0468 ($/kWh)

Figure 7 represents the power resources and the AC primary load. Two points are taken as a presentation of the recorded output production of HES and the power consumed by the primary load. These two points are at 11:00 am on day 30 of May and midnight on the 2 of June. While the absence of the PV at midnight, the total power demand was 1269.12 kW supplied by the grid. On the other hand, at 11:00 am, the output power of the PV exceeds the demand of the AC primary load by 15,785.64 kW. This represents the excess power at that time, sold to the grid. There has been no capacity shortage over the year. Therefore, there is

no unmet load over the year. Table 8 displays the system converter electric parameters and their statistics. The losses of the converter system are the total energy lost in the device, which is the difference between the total amount of the input energy of the converter in DC kWh/yr and the total amount of output energy from the converter in AC kWh/yr

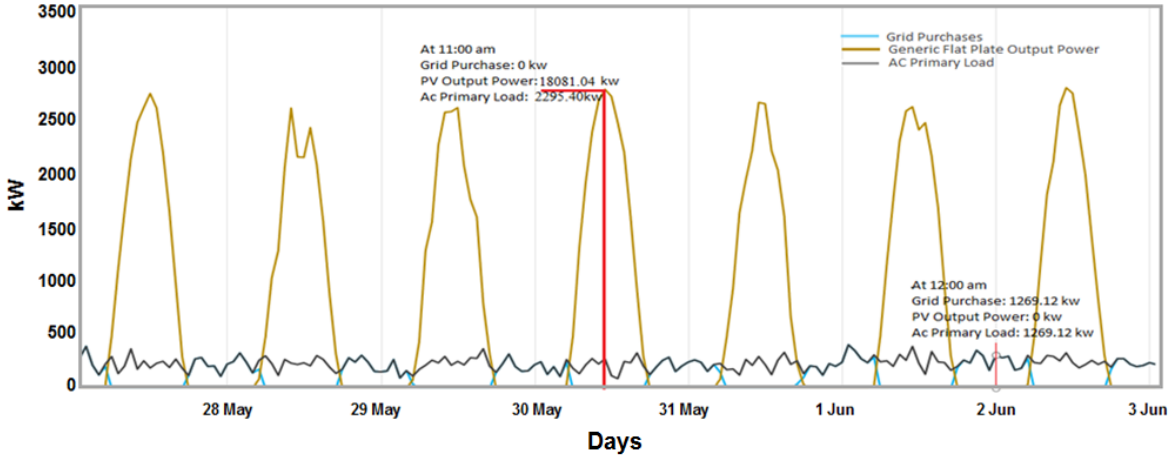

Figure 7: Power Resources and AC Primary Load (Configuration I)

Table 8: Converter Statistics and Output in the Optimal HES (Configuration I)

Quantity	Inverter
Mean output (kW)	4,709
Minimum output (kW)	0
Max output (kW)	14,931
Capacity factor %	31.4
Energy output (kWh/yr)	41,247,657
Energy In (kWh/yr)	43,418,587
Hours of Operations (hrs/yr)	4,373
Losses (kWh/yr)	2,170,929

Moreover, selling power to the grid reduces the total amount of emissions produced. Finally, the emissions from this optimal system that HOMER optimizes are calculated after the simulation by multiplying the emission factors [6] for each pollutant emitted from the system power resource in kg by the total annual fuel consumption. The total annual pollutant emission generated per year by the power system in kg/yr will be illustrated in the comparison section.

The previous simulation was done with a Day-to-day 5% and time-step 10% variability. Three different values of random variability and the resultant parameters are displayed in Table 9. When these values are changed, they affect the size, total NPC, and COE of the HES. By decreasing the variability in the demand power of the electric load, the size of the HES and REF are decreased while the system NPC, COE, and emissions are increased. HOMER credits the HES for these reductions.

Table 9: Random Variability versus System Size, Emissions, NPC, COE, Peak Load, and Load Factor

Random Variability	Peak Load (kW)	Load Factor (%)	Size of PV (kW)	Converter Size (kW)	REF (%)	NPC ($M)	COE ($/kWh)	CO_2 Kg/yr
Day-to-Day 10% Time step 20%	4,297	0.47	34,118	19,338	85.1	6.14	0.0113	5,871,315
Day-to-Day 5% Time step 15%	3,678	0.55	29,026	16,551	83.0	7.05	0.0148	5,895,486
Day-to-Day 5% Time step 10%	3,318	0.61	26,480	14,931	81.5	7.85	0.0172	5,909,888

Day-to-Day0% Time step0%	2,344	0.87	63.7	4.58	0.107	13.25	0.0852	11,264,730

5.3 (Wind-Diesel) Standalone HES:

In such a case, the farm of the selected area is connected to (Wind-Diesel) Standalone HES shown in Figure 8. The size of the WT of the selected type of manufacturer, Generic WT, is optimized by the HOMER optimizer to satisfy the electric demand under certain constraints which is specified in the previous configuration in addition to the operating reserve constraint, which is limited to 50% of the output wind power [43]. After the simulation, it is found that an Auto size generator of 3700 kW (Its rating is the peak of load + 10 % roughly) can satisfy the electric demand of 17,843,025 kWh/yr. The NPC of this configuration is $165,000,000, and the resultant cost of unit energy is 1.06 $/kWh. The total annual average fuel consumption is 4,685,964 L/yr, depending on the generator operational hours, which is 8760 hrs. over the year. The operational life is 1.71 years, affecting the system replacement cost and economics.

Moreover, it has a bad impact on the environment. The total annual production of CO2 is 12,266,049 kg/yr. To include wind energy in the solution, a sensitivity analysis is performed to determine the indefinite amount of the share of wind production in the total average annual electrical power production. The input sensitivity variable is the REF, which describes the amount of energy delivered to the load produced by RERs. Its value has been changed from 0 to 60 % in steps of 10 %.

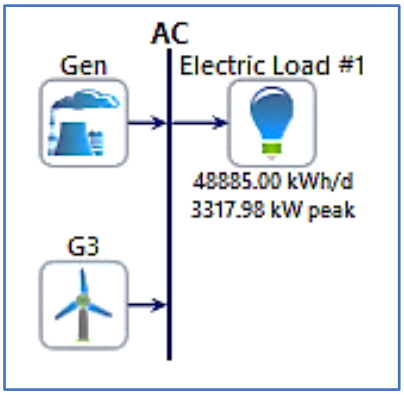

Figure 8: (Wind-Diesel) Standalone HES (Configuration V)

HOMER suggests the suitable, feasible architecture for a HES with 0 % or 10 % or 20 %...etc. of a REF, as seen in Table 10which displays the systems' NPC, COE, CO2, and optimal sizing for sensitivity inputs of the REF in the case of (Wind-Diesel) standalone HES. The least system NPC ranks results, and then HOMER optimizes each sensitivity case separately. From Table 10 for a REF of 0%, the suggested system sizing is Auto size generator of 3700 kW. Additionally, the suggested system size for 0.377% of REF is Auto size generator of 3700 kW and 21 units of WTs of 3 kW rated (total rated capacity of the WT is 21*3 kW = 63kW) and so on for other values of REF.

The optimal solution for the least NPC is the system with REF of 30 %, NPC of $165,250,900, and COE of 1.06 $/kWh. However, the system with the least CO_2 emissions is the configuration with 60 % REF of only 4,348,178 kg/yr of CO_2 pollutants. After sensitivity analysis, the resultant optimal configuration is obtained at 30 % REF. The optimal solutions for sizing the system components at 30 % REFs are shown in Table 11.

Table 10: Sensitivity Cases (Configuration V)

REF (%)	Wind (3 kW unit)	Autosize(kW)	NPC ($)	COE ($/kWh)	O&M ($/yr)	Initial capital ($)
0	0	3700	1.65E+08	1.0615	1.89E+07	740000
0.3773	21	3700	1.65E+08	1.0619	1.89E+07	845000
10	3395	3700	1.65E+08	1.0625	1.69E+07	1.77E+07
10	3480	3700	1.65E+08	1.0631	1.69E+07	1.81E+07
20	3565	3700	1.65E+08	1.0633	1.68E+07	1.86E+07
20	3735	3700	1.65E+08	1.0634	1.67E+07	1.94E+07
30	4329	3700	1.65E+08	1.0629	1.64E+07	2.24E+07
30	4414	3700	1.65E+08	1.0630	1.63E+07	2.28E+07
40	8318	3700	1.72E+08	1.1061	1.49E+07	4.23E+07

40	8403	3700	1.72E+08	1.1078	1.49E+07	4.28E+07
50	17187	3700	2.02E+08	1.2965	1.32E+07	8.67E+07
50	17315	3700	2.02E+08	1.2999	1.32E+07	8.73E+07
60	48888	3700	3.44E+08	2.2143	1.14E+07	2.45E+08

Table 11: Optimal HESs for REF 30 % (Configuration V)

Wind (kW)	Autosize(kW)	NPC ($)	COE ($/kWh)	O&M ($/yr)	Initial capital ($)	REF (%)	Total Fuel (L/yr)	CO_2 (kg/yr)
4329	3700	1.65E+08	1.0629	1.64E+07	2.24E+07	30.7275	3333777	8726545
4414	3700	1.65E+08	1.0630	1.63E+07	2.28E+07	31.00629	3320790	8692550
4498	3700	1.65E+08	1.0633	1.63E+07	2.32E+07	31.27426	3308314	8659891
4583	3700	1.65E+08	1.0633	1.63E+07	2.37E+07	31.55068	3295372	8626015
4244	3700	1.65E+08	1.0636	1.65E+07	2.20E+07	30.40908	3348813	8765901
4753	3700	1.66E+08	1.0650	1.62E+07	2.45E+07	32.02344	3273621	8569080
5093	3700	1.66E+08	1.0662	1.60E+07	2.62E+07	33.03629	3226253	8445088
5432	3700	1.66E+08	1.0677	1.58E+07	2.79E+07	33.9974	3181172	8327083
6111	3700	1.67E+08	1.0753	1.56E+07	3.13E+07	35.62105	3105752	8129664
6790	3700	1.69E+08	1.0840	1.54E+07	3.47E+07	37.10125	3036807	7949190
8148	3700	1.72E+08	1.1033	1.49E+07	4.15E+07	39.71418	2914414	7628814

The total energy production of the system power resources supplies the total average electrical demand of 17,843,025 kWh/yr. Besides, an average annual excess electricity of 8,394,152 kWh/yr, which represents 32% of the total annual energy production, is also available. The REF is 30.7 %, with maximum renewable penetration of 973 %; that is high enough to cause stability problems. This system is reliable with no unmet electrical load and no losses in the converter as it is not used. Therefore, adding some form of storage such as a flywheel or battery bank or using thermal load is recommended.

The excess electricity is produced from either sources or one of them, namely WT or generator. In Figure 9, the excess of electricity in the time step 3:00 pm of the day the 24 of May presents 85.1 % of the total power output, which is not used in serving the demand. Moreover, when the wind output power is zero, the generator operates to serve the load, as shown in step 4:00 on the 19 of May. Therefore, it is recommended to add a storage component that leads to a decrease in the cost of unit energy.

The output power of the generator over the year and its statistics are listed in Table 12. The total annual average fuel consumption is 3,333,777 L/yr, while the average fuel consumed per day is 9,134 L/d, and the average fuel consumed per operation hour is 381 L/hr.

Table 13 displays the mean, the minimum, and maximum output power of the Generic 3kW WT over a year. The capacity factor of the WT is (1,584/12,987 = 12 %) while the wind penetration equals (1,584/2036.8 = 77.8 %).Table 14 displays the emissions produced by the system. The optimal solution (minimum NPC) is for the configuration of 30% REF, while obtaining the least system emissions is for the system of 60% REF but with high NPC.

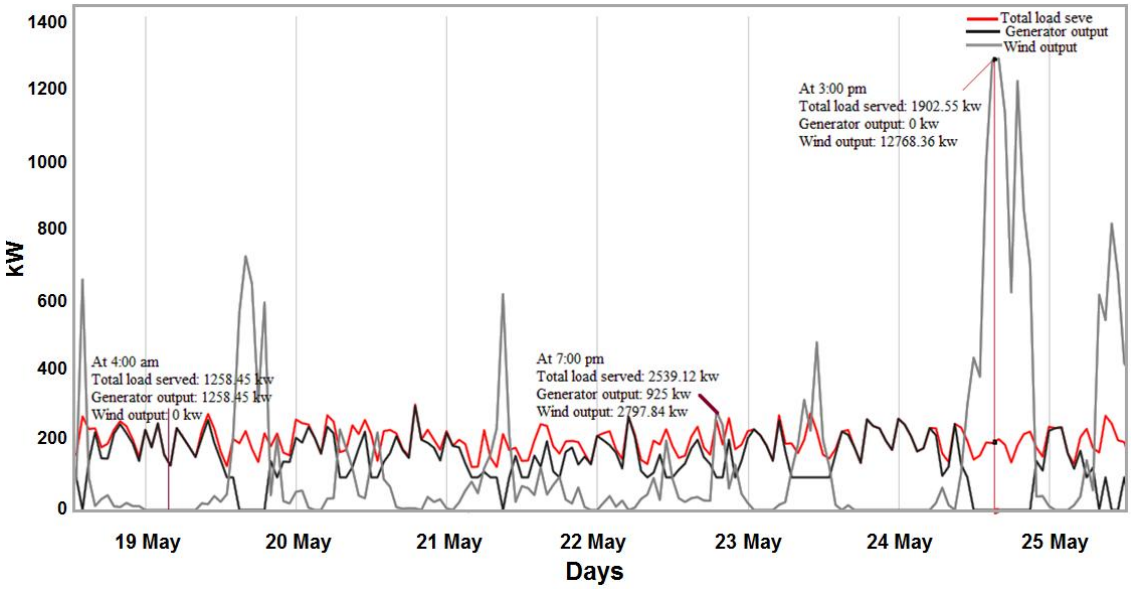

Figure 9: Power Resources Output of the Optimal HES and Load Served (Configuration V)

Table 12: The Electric Generator Output Summary (Configuration V)

Hours of operation (hr/yr)	7684
Number of starts (start/yr)	386
Operational life (yr)	1.95
Capacity factor %	38.1
Mean electrical output (kW)	1609
Minimum electrical output (kW)	925
Maximum electrical output (kW)	3269

Table 13: WT Electrical Summary and Statistic Parameter (Configuration V)

Min. Output (kW)	0
Max. Output (kW)	12,987
Mean output (kW)	1,584
Wind Penetration (%)	77.8
Capacity Factor (%)	11.8
Hours of operation (hrs/yr)	6,506
Levelized Cost ($/kWh)	0.192

Table 14: System Emissions (Configuration V)

Carbon Dioxide (kg/yr)	8,726,545
Carbon Monoxide (kg/yr)	55,007
Unburned Hydrocarbon (kg/yr)	2400
Particulate Matter (kg/yr)	333
Sulfur dioxide (kg/yr)	51,674
Nitrogen oxides (kg/yr)	27,265

5.4 (Wind-Battery) Standalone HES:

In such a case, the farm of the selected area is connected to (Wind-Battery) Standalone HES shown in Figure 10. When HOMER simulates the system to get the optimal feasible system, the solution was "No Feasible Solution Found."

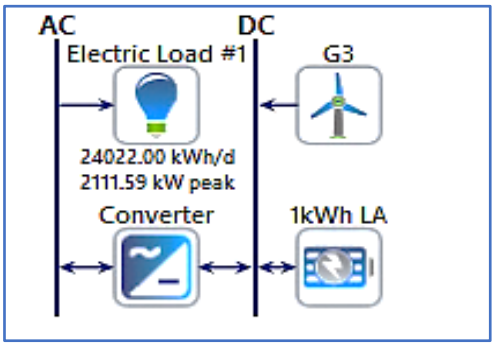

Figure 10: (Wind-Battery) Standalone HES (Configuration VI)

HOMER was unable to find a system that meets the demand because of the following reasons:

- Not enough generation capacity.
- The maximum allowed annual capacity shortage is not satisfied.
- Minimum renewable energy fraction.

Adding additional generation such as diesel and/or PV panels to this configuration is recommended. However, a sensitivity analysis, search space, and optimization are done to find the feasible solution for this configuration. The sensitivity analysis is done for the system's maximum annual capacity shortage constraint and the WT hub height. Subsequently, HOMER simulates all feasible solutions to optimize the allowable limit of maximum shortage over the year and the optimal hub height. Moreover, a search space is done for the number of Generic 3 kW WT, but the HOMER optimizer optimizes the sizes of the converter and battery.

Table 15 displays the sensitivity input values of the maximum annual capacity shortage and the rotor height of the WT. The search space for the number of WTis0, 1000, 1500, 2000, 2500, 3000, 3500, 4000, and 4500. After the simulation, the feasible solution is based on the Hub height of 100 meters, and the maximum annual capacity shortage is 30 %. This solution is optimized to select the optimal sizing of battery, converter, and the number of a WT that satisfy the system constraints based on the least NPC. The optimal HES sizing of the system components and the system cost summary are displayed in the comparison section. The comparison section also illustrates the power system's total average production and load consumption over the year.

Table 15: Sensitivity inputs of the (Wind-Battery) Standalone HES (Configuration VI)

Max. Annual capacity shortage (%)	10	15	20	25	30
Hub height (m)	17	25	30	50	100

Although there is an excess of electricity, there is an unmet electric load. This is because the excess electricity is produced at a certain time when the batteries are fully charged and cannot absorb the excess. Additional storage is needed to absorb this excess electricity, which will raise the system costs and COE, but the unserved load percentage will decrease in this case. The system losses are 1,955,516 kWh/yr caused by the system converter and the battery. Figure 11 shows the AC primary load served and the unmet electric load. Optimal power resources and AC load served in this configuration are shown in Figure 12. The capacity shortage fraction constraint is given in equation (20).

From Figs.11 and 12, at a time step, 2:00 am on the 17 of November, the battery state of charge is 99.9 %, and the output of WT is 13,200.10 kW. This output power serves the load demand of 2432.19 kW and charges the battery with an input power of 27.1 kW. The excess of electricity, at this time step, is 10,612.8 kW and the total losses produced by the converter and DC bus is 128.01 kW. But at a time step, 1:00 am on the 15 of November. The WS is 0.91 m/s. Therefore, the WT output power is zero kW, and the BSS's SOC is 40 %. This is the minimum SOC below it. The BSS is never drawn. Therefore, the capacity shortage is 20428.86 kW, and the unmet load is 2989.82 kW.

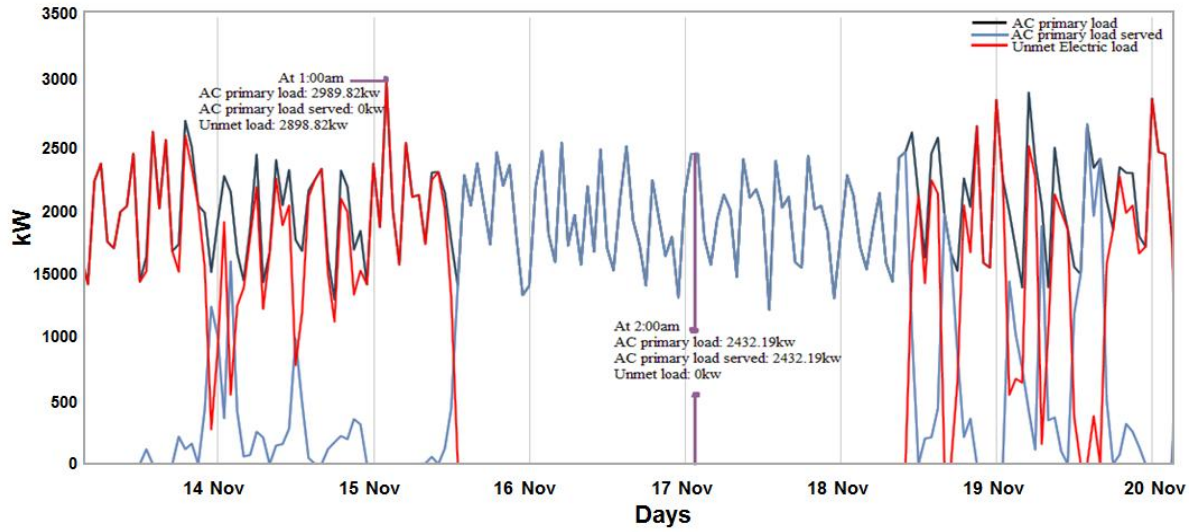

Figure 11: AC Served Load and Unmet Load (Configuration VI)

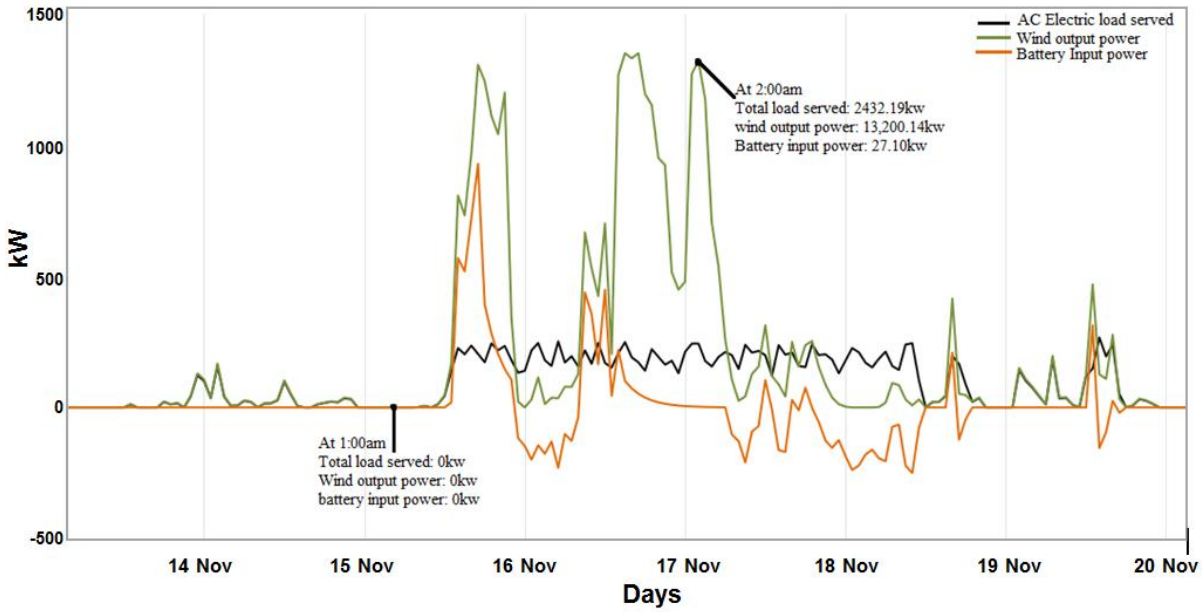

Figure 12: Optimal Power Resources and Served Load (Configuration VI)

The electrical power output and statistics of the system power components are displayed in Tables 16-18. The expected lifetime of the battery is 8.62 years. This system is called a clean system configuration, where it produces no pollutant emissions. This system has low reliability because of the system capacity shortage and has high NPC compared to the previous configurations.

Table 16: Generic 3 kW WT Output Power and Statistics (Configuration VI)

Capacity (kW)	Mean output (kW)	Min. output (kW)	Max. output (kW)	Capacity factor (%)	Annual production (kWh/yr)	REF (%)	Hours (hr/yr)	Levelized cost ($/kWh)
13,500	2,655	0	13,500	19.7	23,262,165	130	7,070	0.119

Table 17: Lead-Acid 1kWh Battery Electric Summary and Statistics (Configuration VI)

Nominal capacity (kWh)	Usable capacity (kWh)	Autonomy (hr)	Storage depletion (kWh/yr)	Total annual losses (kWh/yr)	Annual throughput (kWh/yr)	Lifetime throughput (kWh)	Storage wear cost ($/kWh)
61,901	37,141	18.2	37,141	1,279,151	5,740,144	49,481,600	0.419

Table 18: System Converter Outputs and Statistics (Configuration VI)

Capacity (kW)	Mean output (kW)	Min. output (kW)	Max. output (kWh/day)	Capacity factor (%)	Hours of operation (hr/yr)	Annual energy output (kWh/yr)	Annual enegy input (kWh/yr)	Annual losses (kWh/yr)
3,518	1,548	0	3,318	44	8,284	13,556,610	14,270,116	713,506

VI. COMPARATIVE RESULTS AND DISCUSSIONS

After simulating and optimizing each configuration to satisfy the farm load consumption over the project lifetime, each configuration has its merits and demerits based on the system's total NPC, COE, reliable resources, energy balance, and environmental effects. To analyze the merits and demerits of all the considered configurations, comparison tables and charts of all the studied cases are carried out. Tables 19 to 21 are the comparison based on the optimal capacity sizing, cost, emission summary, and electric production summary, respectively. Despite that, the solar energy for the selected project area is available yet abundant; the standalone (PV) system requires a large storage system, where it is recorded that the large storage system of 90,197 kWh is associated with (PV-Battery) HES as displayed in Table 19. Carbon dioxide (CO_2) is superior to other pollutant factors. The diesel generator is considered a backup source when integrated into the HESs. The standalone (diesel) generator is a reliable source. Yet, it recorded an expensive NPC of \$165 E 06 and COE of 1.06 \$/kWh.

Moreover, it is the most recorded pollutant system. Therefore, by integrating the (PV) system with the standalone (diesel) generator, the greenhouse gases are extremely reduced (CO_2 is reduced from 12,266,049 kg/yr to 7,335,550 kg/yr). Moreover, when the Diesel generator is added to the (PV-Battery) standalone HES, the size of the battery is reduced. Consequently, the percentage of fuel-saving is increased by increasing RER capacity.

Table 19: Optimal Capacities of Different Resources for the Twelve Configurations

Configuration #	PV Capacity (kW)	Wind Capacity (kW)	Diesel Capacity (kW)	Battery Capacity (kWh)	Maximum Grid Power (kW)
I	26,480	-	-	-	3,318
II	38,680	-	3,700	-	-
III	24,206	-	-	90,197	-
IV	18,153	-	3,700	60,359	
V	-	12,987	3,700	-	-
VI	-	13,500	-	61,852	-
VII	-	22,401	3,700	72,616	-
VIII	37,304	5,982	3,700	-	-
IX	22,586	3,726	-	75,077	-
X	15,320	2,427	3,700	61,893	-
XI	26,480	0	-	-	3,318
XII	-	0	-	-	3,318

Table 20: Cost and Environmental Effect for the Twelve Configurations

Configuration #	Capital Cost (M$)	NPC(M$)	M & O (M$/yr)	COE ($/kWh)	Simple Payback (year)	CO_2 emitted (Kg/yr)
I	23.0	7.58	- 1.77	0.0172	6.79	5,909,888
II	28.8	139.5	12.7	0.897	4.55	7,335,550
III	45.1	70.1	2.87	0.451	5.01	0
IV	44.7	96.3	5.92	0.619	2.4	287,746
V	22.4	165.3	16.4	1.0629	6.64	8,726,545

VI	42.1	54.94	1.47	0.4651	-	0
VII	62.40	124.80	7.16	0.8027	4.7	3,312,488
VIII	37.90	142.2	11.97	0.9144	-	6,302,031
IX	45.7	67.95	2.55	0.4373	6.1	0
X	35.1	63.67	3.28	0.4095	1.9	219,941
XI	23.0	7.58	-1.77	0.0172	6.79	5,909,888
XII	0	13.2	1.52	0.085	-	11,276,790

Table 21: Energy Production and Consumption for the Twelve Configurations

Configuration #	Production (kWh/yr)	Served Load (kWh/yr)	Excess Electricity (kWh/yr)	Unmet Load (kWh/yr)	Shortage (kWh/yr)	REF (%)
I	54,834,304	50,598,746	32,755,721	0	0	81.5
II	76,941,732	17,843,025	58,712,406	0	0	41.1
III	41,578,120	17,829,342	20,362,840	13,683	17,634	100
IV	31,592,546	17,843025	10,423,788	0	0	97.7
V	26,237,177	17,843,025	8,394,152	0	0	30.7
VI	23,262,164.89	13,556,610.22	7,750,039	4,286,415	5,369,801	100
VII	28,692,076	17,843,025	8,977,126	0	0	73.3
VIII	79,375,090	17,843,025	61,284,332	0	0	50.1
IX	42,776,579	17,831,692	22,085,650	11,333	17,810	100
X	29,221,242	17,843,025	8,395,590	0	0	98.2
XI	54,834,304	50,598,746	32,755,721	0	0	81.5
XII	17,843,025	17,843,025	-	0	0	0

The least NPC and COE are achieved if the configuration includes the grid. However, if the farm is isolated from the grid, the system that has the least NPC is the (Wind-Battery) standalone HES (at 100 m Hub height). The merits of this system are the least NPC and no emitted pollutants. Therefore, this system is clean, and its COE is slightly higher than the (PV-Wind-Diesel-Battery) standalone HES, with the least COE of 11.95 %. However, this configuration (Wind-Battery) has 30.1% of the total annual capacity shortage fraction; therefore, the demerit of this configuration is unreliable resources. Moreover, the highest systems' NPC and COE are achieved by the (Wind-diesel) standalone HES of $165.3M and 1.0629 $/kWh.

It is noticed that when the battery is added to the (PV-Wind-Diesel) standalone HES, the system NPC and COE decrease from $142.2 E 06 to $63.67 E 06 and from 0.9144 $/kWh to 0.4095 $/kWh, respectively. That is because the number of starting/stopping of the diesel generator is minimized. That means the problem of the diesel generator's premature wear is reduced, and consequently, its operational lifetime increases. Moreover, the configuration of (Diesel) standalone system is the most pollutant system.

The highest production of emissions achieved by the (Diesel) generator followed by the grid, then the (Wind-Diesel) standalone HES of 12,266,049 kg/yr , 11,276,790 kg/yr and 8,726,545 kg/yr , respectively. The lowest emissions system is (PV-Wind-Battery) standalone HES, less than the Diesel generator, Grid and (Wind-Diesel) by 98.21%, 98.05%, and 97.48%, respectively. On the other hand, the standalone configurations that do not include a diesel resource are called clean systems with no emissions.

From the emissions of the system in Table 20, it is noticed that the least systems' production of emission is in (PV-Battery), (Wind-Battery), and (PV-Wind-Battery) standalone HESs (configurations III, VI, and IX). These three systems are called clean systems. But these systems are unreliable, as shown in Figure 13, as there are capacity shortages in these HESs. The unreliable system refers to its intermittent nature. Total annual capacity shortages of the three configurations are 17,634 kWh/yr, 5,369,801kWh/yr, and 17,810 kWh/yr, respectively. Moreover, the highest percentage is 30% achieved by the (Wind-Battery) standalone HES, and the least percentage is 0.0635% achieved by the (PV-Wind-Battery) standalone HES.

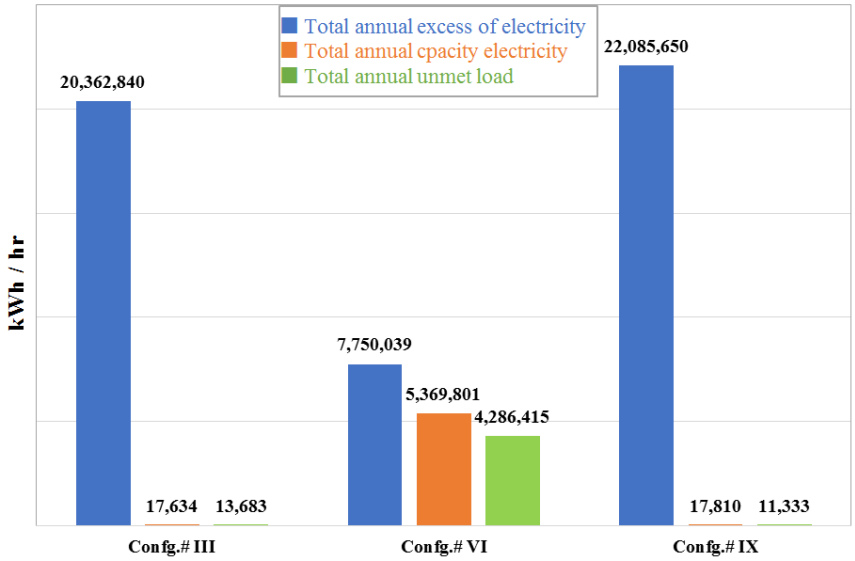

Figure 13: The System Reliability for Clean HESs

The least annual excess of electricity is achieved by (Wind-battery) standalone HES with a 30 % maximum allowable capacity shortage fraction. In contrast, the highest production is achieved by (PV-Wind-Diesel) standalone HES. It is noticed that the (PV-Wind-Diesel) standalone HES has a total annual excess of electricity higher than the (Wind-Battery) standalone HES by 87.35 %. Therefore, the (PV-Wind-Diesel) standalone HES'NPC and COE are higher than (Wind-Battery) standalone HES by 61.34 % and 49.14 %, respectively. This means that excess electricity affects the system's economics and stability. Therefore, achieving a reliable system with the least NPC and COE and as much as possible is important to achieve the least emission production is important. Therefore, this study is not only based on the least total NPC of the system, but also it is important to study the effect of the systems on the environment, system reliability, and stability to decide which the optimal configuration that satisfies the total annual electric load and system's constraints.

VII. APPLICATION OF TOPSIS DECISION SUPPORT METHOD

TOPSIS is a multi-criteria decision analysis method that ranks the alternatives based on various criteria [45 - 47]. It is also applied to the case study to rank the bases of the different systems on the main objective functions (Eq.9), Levelized Cost of Energy (Eq.12), Unmet Load, and CO_2 emitted as the main criteria of the decision. The results are summarized in Table 22. The Symbols S_j^+, S_j^-, V_j^+, V_j^-, and P_i are defined in [45,47]. The performance score P_i, used to rank the system performance, decides the best result for the system X ((PV-Battery-Wind-Diesel) Standalone HES) as achieved by HOMER Software.

Table 22: TOPSIS Results

Config. #	NPC (M$)	Unmet load (kWh/yr)	COE ($/kWh)	CO_2 emitted (Kg/yr)	S_j^+	S_j^-	$(S_j^+) + (S_j^-)$	P_i
I	0.00574647	0	0.0020083	0.0760129	0.076012894	0.31059349	0.3866064	0.80338428
II	0.10575636	0	0.1047344	0.0943497	0.171628977	0.25656657	0.4281956	0.59918085
III	0.05314352	0.000798	0.0526591	0	0.16077866	0.30569761	0.4664763	0.65533368
IV	0.073006	0	0.0722749	0.003701	0.097339306	0.29647738	0.3938167	0.75283093
V	0.1253156	0	0.124105	0.1122407	0.204456257	0.25214053	0.4565968	0.55221705
VI	0.04165057	0.2499979	0.0543054	0	0.257920573	0.18140831	0.4393289	0.41292143
VII	0.09461214	0	0.0937239	0.0426052	0.134625611	0.27360177	0.4082274	0.67021906
VIII	0.10780325	0	0.106766	0.0810566	0.167212296	0.27981907	0.4470314	0.62594952
IX	0.05151358	0.000661	0.0510595	0	0.067090125	0.30657531	0.3736654	0.82045402
X	0.04826887	0	0.0478135	0.0028289	0.062564186	0.30737609	0.3699403	**0.83088031**

XI	0.00574647	0	0.0020083	0.0760129	0.076012894	0.31059349	0.3866064	0.80338428
XII	0.01000705	0	0.0099247	0.1450419	0.145320257	0.29804721	0.4433675	0.67223518
$\mathbf{V_j^+}$	0.00574647	0	0.0020083	0				
$\mathbf{V_j^-}$	0.1253156	0.2499979	0.124105	0.1450419				

VIII. CONCLUSIONS

The optimization of RES in HES is a multiobjective topic that deals with economic, technical, and environmental issues, as the optimal components depend on available RERs at load location. This study examines the techno-economic and environmental feasibility analysis based on certain key performance, such as system NPC, COE, sensitivity inputs, the contribution of RERs, and environmental effect. The study formulates the optimization problem and develops the equality and inequality constraints that the solution must satisfy. The Proposed procedure for the problem solution is based on the Solving Tool "HOMER" Software. It is applied to a selected project at Upper Egypt to verify the procedure. In case of no feasible solution to supply the load for certain configuration components, the constraints may be relaxed through sensitivity analysis to get a compromise solution.

For a standalone HES system, it is preferable to utilize batteries than Diesel engines, despite their high capital cost. This is because of a smaller number of replacements due to aging; moreover, it is environmentally friendly. Adding Batteries to HES reduces the system's size of (PV) and WT. In the selected area, wind energy is not superior to resources due to its weak availability related to low average WS. This causes high COE. The least COE is from the PV panels. Therefore, the priority of supplying the load demand goes to the (PV) Grid-Connected HES. It is deduced that for the studied location, the height of the hub of the wind tower is to be 100 meters to have an acceptable solution for supplying power of wind energy to the load.

Further, (PV) Grid-Connected HES is a reliable system that can meet the total annual electric demand (farm demand or the grid sale). This configuration produces a total annual electric production of 45,834,304 kWh/yr with a REF of 81.5%. This system has the least NPC and COE values, \$7.85E+06 and 0.0172 \$/kWh, respectively, and the payback is 6.8 years. The most feasible and optimal standalone configuration is the (PV-Wind-Diesel-Battery) standalone HES. It records the minimum CO_2 emissions of 219,941 kg/yr, a minimum recovery period of 1.9 years, the excess electricity of 8,395,590 kWh/yr, and the REF of 98.2 %. On the other hand, it is recommended to study the effect of adding thermal load, applying demand-side management, and the effect of electric load growth within the project lifetime on the system economics and stability as future research.

REFERENCES

[1]. M. Katsivelakis, D. Bargiotas, A. Daskalopulu, I. P. Panapakidis, L. Tsoukalas, Techno-Economic Analysis of a Standalone Hybrid System: Application in Donoussa Island, Greece, Energies, 14, (2021) 1868.

[2]. J. Ahmed, K. Harijan, P. H. Shaikh, A. A. Lashari, Techno-economic Feasibility Analysis of an Off-grid Hybrid Renewable Energy System for Rural Electrification, Journal of Electrical and Electronic Engineering, 9; 1 (2021) 7-15.

[3]. S.M. Shaahid, Review of research on autonomous wind farms and solar parks and their feasibility for commercial loads in hot regions, Renew. Sust. Energ. Rev. 15; 8 (2011) 3877-3887.

[4]. A. Acakpovi, E.B. Hagan, F.X. Fifatin, Cost Optimization of an Electrical Energy Supply from a Hybrid Solar, Wind and Hydropower Plant, Int. J. Comput. Appl. 114; 19 (2015) 44-51.

[5]. M.A. Hessami, Designing a hybrid wind and solar energy supply system for a rural residential building, Int. J. Low-Carbon Tec. 1;2 (2006) 112-126.

[6]. A. Naeem, NU. Hassan, C. Yuen, S.M. Muyeen, Maximizing the economic benefits of a grid-tied microgrid using solar-wind complementarity, Energies 12;3 (2019) 1-22.

[7]. NH. Samrat, N. Ahmad, I.A. Choudhury, Z. Taha, Technical Study of a Standalone Photovoltaic-Wind Energy Based Hybrid Power Supply Systems for Island Electrification in Malaysia, PLoS One 10;6 (2015) 1-35.

[8]. P. E. Bett, H. E. Thornton, The climatological relationships between wind and solar energy supply in Britain", Renew. Energ. 87;1 (2016) 96-110.

[9]. M. Abdel-Salam, A. Ahmed, H. Ziedan, K. Sayed, M. Amery, M. Swify, A solar-wind hybrid power system for irrigation in toshka area, IEEE Conf. on App. Elec. Eng. and Comp. Tec., Jordan (2011) 1-6.

[10]. SK. Nandi, H.R. Ghosh, Prospect of wind-PV-battery hybrid power system as an alternative to grid extension in Bangladesh, Energy 35;7 (2010) 3040-3047.

[11]. S. Ahmed, H. Othman, S. Anis, Optimal sizing of a hybrid system of renewable energy for a reliable load supply without interruption, European J. of Scient. Res. 45;4 (2010) 620-629.

[12]. S. Kahrobaee, S. Asgarpoor, M. Kahrobaee, Optimum renewable generation capacities in a microgrid using generation adequacy study, IEEE Conf. Exp., USA (2014) 1-5.

[13]. M. Zahran, A. Yousef, Monitoring of photovoltaic wind-turbine battery hybrid system, WSEAS Trans. Power Syst. 9 (2014) 7-15.

[14]. JA Razak, K. Sopian, Z.M. Nopiah, A. Zaharim, Y. Ali, Optimal operational strategy for hybrid renewable energy system using genetic algorithms, Proceeding of WSEAS Int. Conf. on App. Math., Egypt (2007) 235-240.

[15]. R. Belfkira, G. Barakat, T. Nicolas, C. Nichita, Design study and optimization of a grid independent wind/PV/Diesel system, Proc. of the 13th European Conf. on Power Elect. & App., Spain (2009) 1-10.

[16]. L. Zhang, R. Belfkira, G. Barakat, Wind/PV/diesel energy system: Modeling and sizing optimization", Proc. of European Conf. on Power Elect. & App., UK (2011) 1-10,
[17]. S. Wen, H. Lan, Q. Fu, D.C. Yu and L. Zhang, Economic Allocation for Energy Storage System Considering Wind Power Distribution, IEEE Trans. on Power Syst. 30;2 (2015) 644-652.
[18]. M. Combe, A. Mahmoudi, M.H. Haque and R. Khezri, Cost-effective sizing of an AC mini-grid hybrid power system for a remote area in South Australia, IET Gener. Transm. Distrib. 13;2 (2019) 277-287.
[19]. T. Adefarati1, G.D. Obikoya, Assessment of Renewable Energy Technologies in a Standalone Microgrid System, Int. J. Eng. Res. Africa 47 (2020) 146-167.
[20]. T. Adefarati, G.D. Obikoya, Evaluation of Wind Resources Potential and Economic Analysis of Wind Power Generation in South Africa, Int. J. Eng. Res. Africa 44 (2019) 150-181.
[21]. A. Souissi, An Accurate Optimal Sizing Method of a Hybrid PV/Wind Energy Conversion System with Battery Storage, Int. J. Eng. Res. Africa 48 (2020) 179-192.
[22]. MA Abdelkader, M.A. Elshahed, Z.H. Osman, A New Power Flow Algorithm for Passive and Active Radial Distribution Networks, Int. J. of Eng. Res. in Africa 40 (2018) 101-118.
[23]. A.H. Shehata, A.A. El-Deib, Z.H. Osman, New Approach of Calculation the Steady State Symmetrical Fault Current for Type 4 Wind Power Plants, Int. J. Eng. Res. Africa 48 (2020) 162-178.
[24]. M. Elshahed, M. Dawod, Z.Osman, Optimization of Real Power Loss and Voltage Stability Index of Distribution Systems with Distributed Generation, Int. J. Eng. Res. Africa 33 (2017) 100-114.
[25]. Available Online: https://www.homerenergy.com/products/pro/docs/latest/index.html
[26]. J.A. Duffie, W. A. Beckman, Solar Engineering of Thermal Processes, 2nd edition, New York, Wiley Interscience, 1991.
[27]. C. Phurailatpam, B. S. Rajpurohit, L. Wang, Planning and optimization of autonomous DC microgrids for rural and urban applications in India, Renew. and Sust. Ener. Rev. 82 (2018) 194-204.
[28]. Wind Characteristic and Resources. Available Online: http://www.winddata.com
[29]. J.F. Manwell, J.G. McGowan, A.L. Rogers, Wind energy explained: theory, design and application, John Wiley & Sons, 2010.
[30]. L. Jiaxin, W. Wang, Y. Zhang, S. Cheng, Multiobjective optimal design of standalone hybrid energy system using entropy weight method based on HOMER, Energies 10;10 (2017) 1-17.
[31]. F.J. Vivas, A.D. Heras, F. Segura, J.M. Andújar, A review of energy management strategies for renewable hybrid energy systems with hydrogen backup, Renew. and Sust. Ener. Rev. 82 (2018) 126–155.
[32]. N. Garimella, N.K.C. Nair, Assessment of battery energy storage systems for small-scale renewable energy integration, TENCON IEEE region 10 conference (2009) 1-6.
[33]. T. Lambert, P. Gilman, P. Lilienthal, Micropower system modeling with HOMER, Integ. of Alter. Sour. of Ener. 1;1 (2006) 379-385.
[34]. J.F. Manwell, J.G. McGowan, Lead acid battery storage model for hybrid energy systems, Solar Ener. 50;5 (1993) 399-405.
[35]. J.F. Manwell, J.G. McGowan, U. Abdulwahid, K. Wu, Improvements to the Hybrid2 Battery Model, Windpower Conference (2005) 1-22.
[36]. E.A. Al-Ammar et al., Residential Community Load Management Based on Optimal Design of Standalone HRES with Model Predictive Control, IEEE Access 8 (2020) 12542-12572.
[37]. U. Akram, M. Khalid, S. Shafiq, An Improved Optimal Sizing Methodology for Future Autonomous Residential Smart Power Systems, IEEE Access 6 (2018) 5986-6000.
[38]. A.S. Aziz, M.F.N. Tajuddin, M.R. Adzman, M. A. Ramli, Feasibility analysis of PV/diesel/battery hybrid energy system using multi-year module, Intern. J. of Renew. Ener. Res. 8;4 (2018) 1980-1993.
[39]. Y.A. Katsigiannis, P.S. Georgilakis, E.S. Karapidakis, Multiobjective genetic algorithm solution to the optimum economic and environmental performance problem of small autonomous hybrid power systems with renewables, IET Renew. Power Gen. 4;5 (2010) 404-419.
[40]. C.D. Barley, C.B. Winn, Optimal dispatch strategy in remote hybrid power systems, Solar Ener.58;6 (1996) 165-179.
[41]. HOMER Pro 3.13 Software. Available Online:https://www.homerenergy.com/products/pro/index.html/
[42]. Available Online: https://www.cbe.org.eg/en/Pages/default.aspx/
[43]. J. Cottrell, Technical Report: Modeling the feasibility of using fuel cells and hydrogen internal combustion engines in remote renewable energy, National Renewable Energy Laboratory (2003).
[44]. Available Online: https://www1.eere.energy.gov/ba/pba/pdfs/entire_document.pdf
[45]. M. Esfandiari, M. Rizvandi: An application of TOPSIS method for ranking different strategic planning methodology, Management Science Letters 4, (2014) 1445–1448,.
[46]. Robbi Rahim et al: TOPSIS Method Application for Decision Support System in Internal Control for Selecting Best Employees, J. Phys.: Conf. Ser. 1028 012052, (2018).
[47]. M. Panda, A. K. Jagatev: TOPSIS in multi-creteria decision making: A Survey, 2nd International conference on data science and businees analytics, (2018) 51-54.

Appendix A

Table A.1 contains the main data description of the selected project.

Table A.1: Main Data of ALDAHER Project, Egypt

Location	TUSHKA-Al Wadi Al Gadid Desert-New Valley Government– AL DAHRA Agriculture
Latitude	22°56'27.7"N
Longitude	31°27'00.3"E
Area to be irrigated	100000 ACres (30000 ACres were reclaimed)
Irrigation system	Pivot irrigation system
Crops types	1-Medicago Sativa (ALFAFA): planted in 19000 Acres

	2- Palm: planted in 60 ACres
Total consumption rate of water	720,000 m^3/day in summer
	420,000 m^3/day in winter
Maximum Static Head	52.5 m
PIVOT content:	The pivot unit consists of 7 connectors, every 52 meters in length. Based on two-wheeled anchors, which spin with a 15 kW rating electrical motor fixed between them. Each pivot consumes 200 m^3 of water per hour
Pumping Station	Each pump station can supply 1200 m^3 of water per hour.
No. of employee	260 fixed employees + 200 temporary employee